Supporting Information

Adams et al. 10.1073/pnas.1320198111

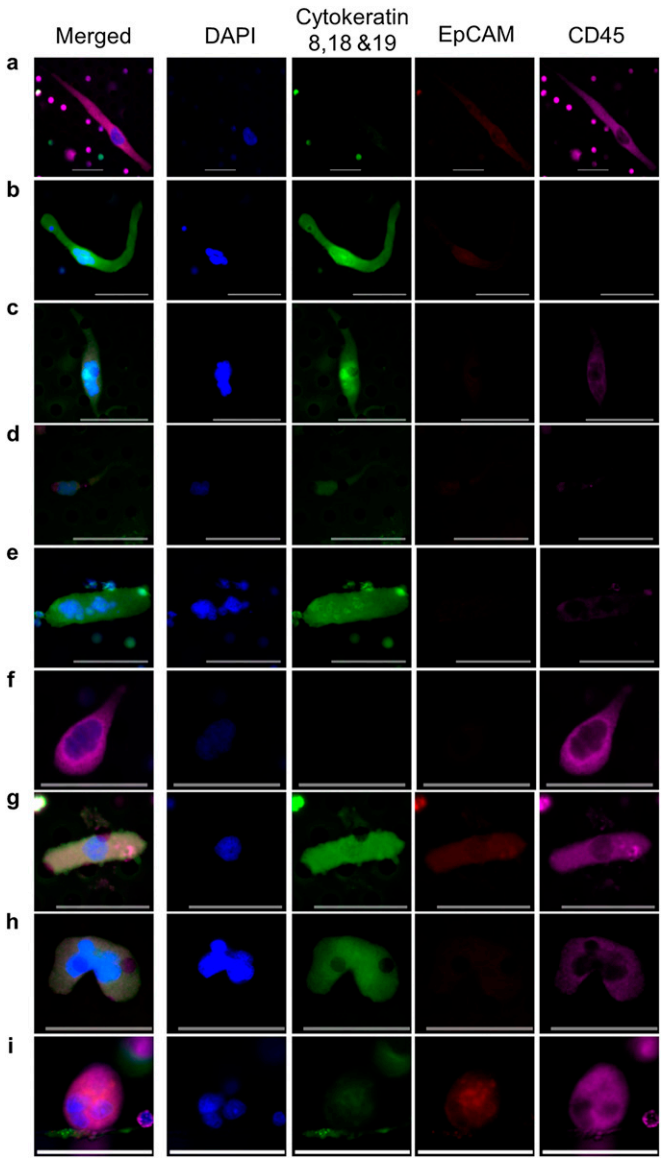

Fig. S1. The individual fluorescent channels from the collage of examples in Fig. 1. Expression of Individual markers can be compared with staining for DAPI (blue), cytokeratins 8, 18, and 19 (green), epithelial cell adhesion molecule (EpCAM) (red), and CD45 (violet). All channels were taken under the same time exposures. (*A*) A spindle-shaped cancer-associated macrophage-like cell (CAML) (prostate) with low levels of cytokeratin/EpCAM expression and high CD45 expression. (*B*) A spindle-shaped cell (breast) with intense cytokeratin and no CD45. A vacuole containing concentrated nucleic acids can be seen as a small, round ball in the far left of the cell. (*C*) A spindle-shaped cell (pancreatic), with an engulfed cell that appears to have epithelium-like cytokeratin expression distinguishable within the nuclear conglomerate. (*D*) A tadpole-shaped cell (prostate) with little to no expression of EpCAM or CD45 and low expression of cytokeratin. (*E*) An oblong cell (pancreatic) with multiple regions of distinct clusters of nucleic acids. (*F*) A tadpole-shaped cell (prostate) with no EpCAM and little cytokeratin expression. (*G*) An oblong cell (breast) with high EpCAM, cytokeratin, and CD45 expression. (*H*) An amorphous-shaped cell (pancreatic) with multiple distinct nuclei. (*I*) A round cell (breast) containing engulfed cytokeratin and EpCAM debris, which is concentrated in the center of the cell. (Scale bars, 50 μm.)

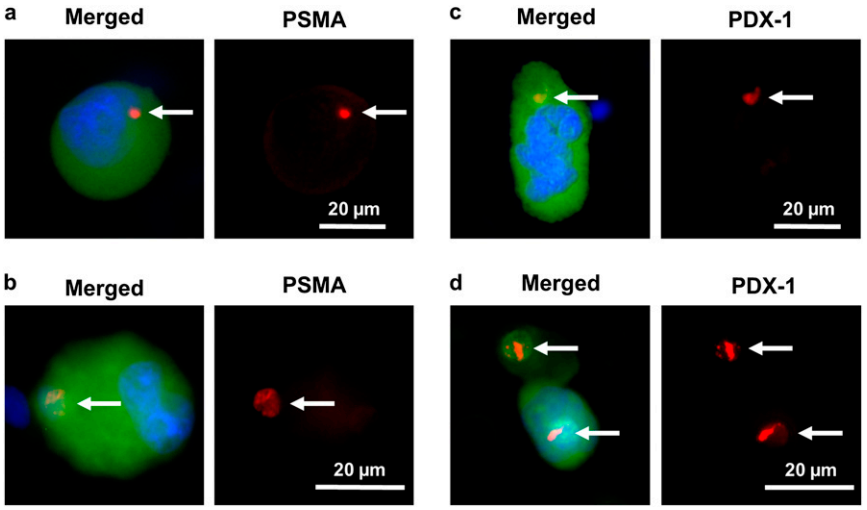

Fig. S2. Examples of CAMLs with internal engulfed prostate-specific membrane antigen (PSMA) and pancreatic duodenal homeobox 1 (PDX-1) debris (*A*) A CAML from a prostate cancer patient stained with DAPI (blue) (*Left*), anti–cytokeratins-FITC (green) (*Left*), and anti–PSMA-Dylight594 (red) (*Left* and *Right*). The arrow indicates PSMA$^+$ debris. (*B*) A CAML from a prostate cancer patient stained with DAPI (blue) (*Left*), anti–cytokeratins-FITC (green) (*Left*), and anti–PSMA-Dylight594 (red) (*Left* and *Right*). The arrow indicates PSMA$^+$ and DAPI-stained debris. (*C*) A CAML from a pancreatic cancer patient stained with DAPI (blue) (*Left*), anti–cytokeratins-FITC (green) (*Left*), and anti–PDX-1-Dylight594 (red) (*Left* and *Right*). The arrow indicates PDX-1$^+$ debris. (*D*) A CAML from a pancreatic cancer patient stained with DAPI (blue) (*Left*), anti–cytokeratins-FITC (green) (*Left*), and anti–PDX-1-Dylight594 (red) (*Left* and *Right*). Arrows indicates PDX-1$^+$ debris. (Scale bars, 20 μm.)

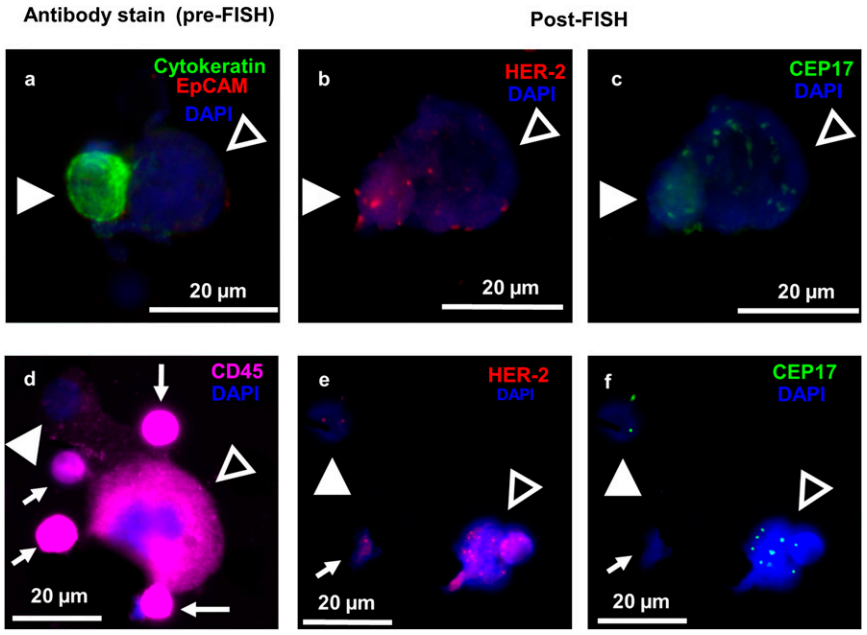

Fig. S3. Examples of CAMLs with engulfed material presenting with HER-2 amplification (*A*) An example of a CAML from a breast cancer patient (open triangle) engulfing a circulating tumor cell (CTC) (solid triangle). Cytokeratin (green), EpCAM (red), and DAPI (blue) are used to identify the CTC. The patient was classified as HER-2–amplified based on standard immunohistochemistry (IHC) histopathology of the primary tumor biopsy. The CAML in this case had weak CD45 expression (Fig. 4C) and weak cytokeratin expression. The CTC has a filamentous cytokeratin staining pattern and is EpCAM$^+$. (*B*) The CTC (solid triangle) appears with eight HER-2 signals (red dots). The CAML (open triangle) appears with 13 HER-2 signals. (*C*) The CTC appears with three chromosome-17 signals (CEP17) (green dots). The HER-2:CEP17 ratio is 2.7, amplified. The CAML (open triangle) appears with 19 CEP17 signals. (*D*) A sample from a breast cancer patient also preidentified as HER-2–amplified based on standard IHC of the primary tumor biopsy. A CAML (open triangle) is shown with CD45 for easy visualization of the engulfment of nuclear material (solid triangle) within the CAML's cytoplasmic border. Four WBCs are labeled with white arrows. (*E*) The engulfed nuclear material (solid triangle) appears with three HER-2 signals. The CAML (open triangle) appears with 16 HER-2 signals. (*F*) The engulfed nuclear material (solid triangle) appears with two CEP17 signals. The CAML (open triangle) appears with nine CEP17 signals. The cells in *A*–*C* were FISH probed after transfer to a microscope slide, and those in *D*–*F* were probed directly on the filter. In both cases many smaller WBC contaminates (white arrows) were digested away by the protease step, leaving only the CAMLs and CTCs. (Scale bars, 20 μm.)

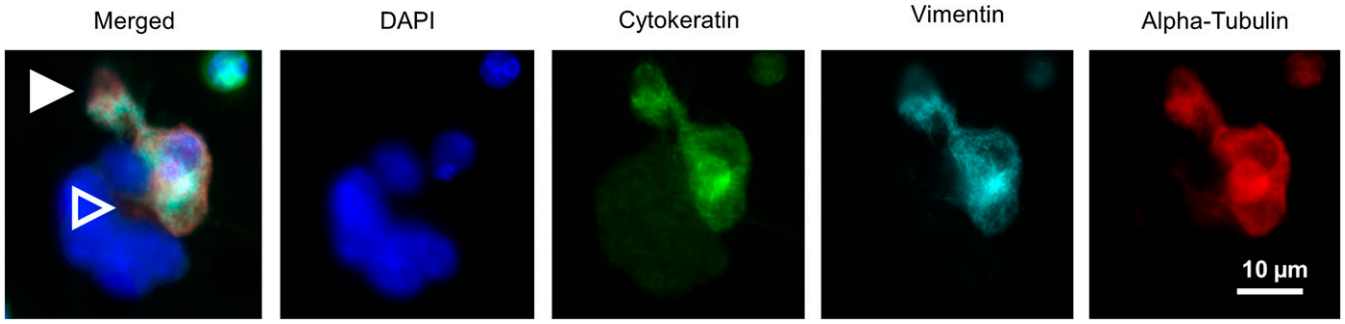

Fig. S4. The cytoskeletal structure of a CTC attached to a CAML imaged by fluorescent microscopy. The cells from a blood sample from a breast cancer patient are isolated on a microfilter. The CTC is highly reactive to cytokeratin (green), vimentin (turquoise), and α-tubulin (red) antibodies, and clear filamentous structures are seen with all three antibodies. The CAML did not have detectable signal for either vimentin or α-tubulin antibody staining but can be distinguished by diffuse cytokeratin signal (green) and the grouping of multiple DAPI-stained nuclei (blue). Filamentous structures protrude out from the CTC above the CAML (solid arrowhead) and into the CAML (open arrowhead). These cells were imaged by a confocal microscope to examine further the putative interaction in 3D (Movie S1). (Scale bar for all images, 10 μm.) The merged image consists of vimentin, α-tubulin, and DAPI.

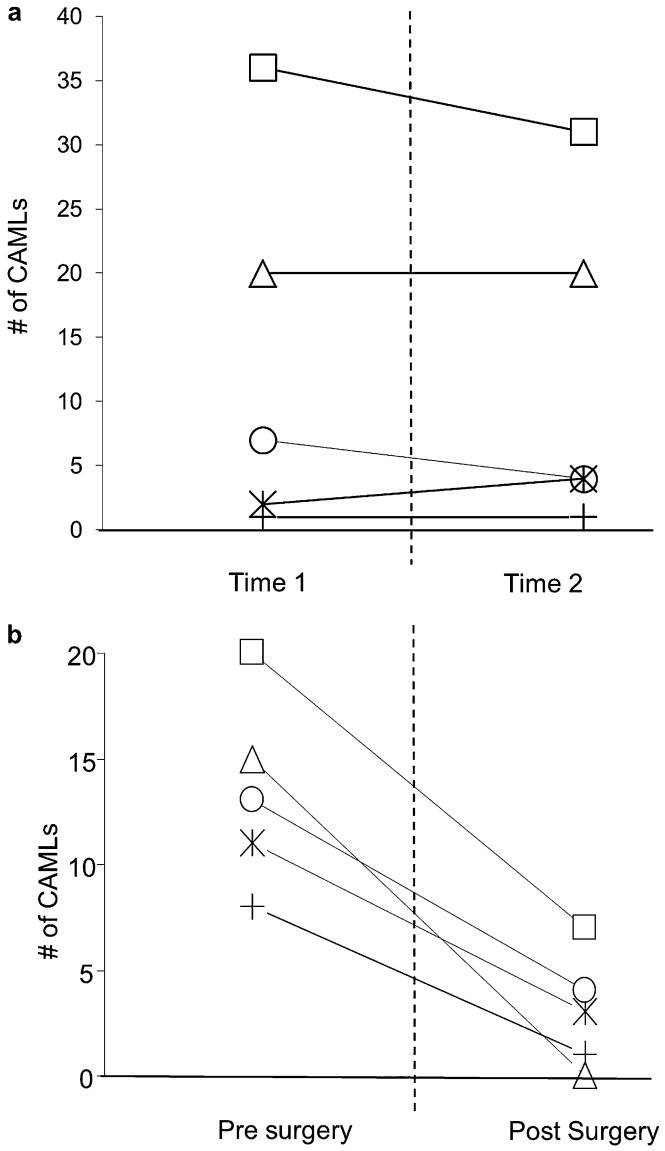

Fig. S5. Comparison of the change in CAML numbers in patients at two surgical or two nonsurgical time points. (*A*) CAMLs were isolated from five individual cancer patients [two with pancreatic cancer (+, *), one with prostate cancer (○), and two with breast cancer (□, Δ)]. At a follow-up visit, 30–180 d later, a second sample was taken before any change in therapy was applied. The number of CAMLs remained steady over various time periods. (*B*) CAMLs were isolated and enumerated from five individual patients with nonmetastatic cancer [three with pancreactic cancer (○, □, Δ) and two with prostate cancer (+,*)] 30–45 d before surgical resection and 30–60 d postsurgical resection. A 65–100% reduction in the number of CAMLs was seen between presurgical counts and postsurgical counts. The reduction, but not complete absence, of CAMLs suggests that the mechanism responsible for the formation of CAMLs is still detectable immediately after surgical cancer resections. A long-term prospective study tracking changes in CAML number in relation to surgical resections is currently underway.

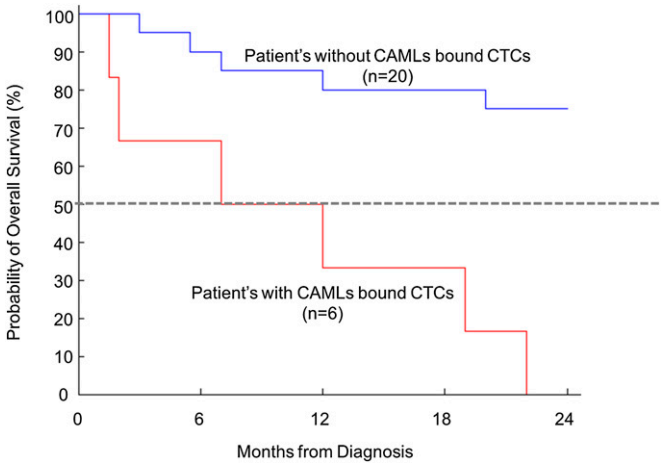

Fig. S6. Preliminary data for the overall survival of patients without a CAML/CTC interaction versus patients with a CAML/CTC interaction. Of the 26 patients on study for at least 24 mo, six had interacting CAMLs and CTCs. Five of these six patients had stage IV cancer, and one of the patients had stage II cancer. Our preliminary findings show that patients with interacting CTCs and CAMLs had a worse prognosis than the remaining patient population ($n = 20$, consisting of one stage I, five stage II, seven stage III, and seven stage IV patients). These preliminary results suggest that a CTC/CAML interaction correlates with worse prognosis. Currently, longer-term tracking of the remaining 79 patients is underway, as is additional patient recruitment to verify this observation.

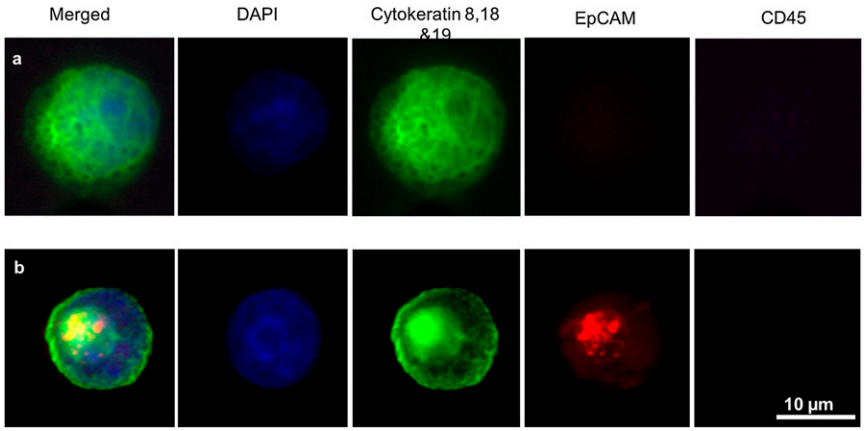

Fig. S7. Examples of CTCs captured on a microfilter isolated from cancer patient blood samples. (*A*) An example of a CTC from a breast cancer patient on a microfilter. The CTC is ~19 μm in diameter, with a cancerous nuclear profile with abnormal chromatin patterns (DAPI, blue), is heavily filamentous (cytokeratin, green), and has no EpCAM (absent, red) or CD45 (absent, violet). (*B*) An example of a CTC from a prostate cancer patient on a microfilter. The CTC is ~15 μm in diameter, with a cancerous nuclear profile with abnormal chromatin patterns (DAPI, blue), is heavily filamentous (cytokeratin, green), is $EpCAM^+$ (red), and has no CD45 (absent, violet). Samples were filtered and stained by the CellSieve assay as described in *Materials and Methods*. (Scale bar for all images, 10 μm.)

Table S1. Summary of healthy subject data, CAML patient data, and CTC patient data separated by stage and therapy type

Disease and treatment characteristics	No. of subjects	CAML$^+$, %	Mean CAML± SD	Median CAML	CAML range	CTC$^+$, %	Mean CTC ± SD	Median CTC	CTC range
Disease status									
Healthy normal	28	0	0 ± 0	0	0–0	0	0 ± 0	0	0–0
Nonmalignant cancer	2	0	0 ± 0	0	0–0	0	0 ± 0	0	0–0
Stage I	12	67	8.6 ± 17.2	3.0	0–61	33	3.3 ± 9.7	0	0–34
Stage II	18	94	7.8 ± 7.8	4.5	0–28	39	5.8 ± 19.4	0	0–83
Stage III	13	100	14.8 ± 12.4	8.0	2–43	62	12.2 ± 29.1	3.0	0–108
Stage IV	24	96	22.0 ± 24.0	10.5	0–82	75	59.7 ± 175.9	3.0	0–682
Unknown	12	100	7.2 ± 3.1	6.5	3–12	50	1.3 ± 1.7	0.5	0–5
Treatment									
No treatment	35	85	4.8 ± 4.9	3.0	0–20	36	4.9 ± 16.3	0	0–83
Hormone	12	92	7.4 ± 5.9	7.0	0–20	70	6.8 ± 9.8	3.0	0–34
Chemotherapy	24	100	26.0 ± 22.0	25.0	2–82	58	9.2 ± 23.1	2.0	0–108
Unknown	8	100	21.4 ± 20.8	12.5	13–64	86	154.1 ± 284.8	2.0	2–682
Total patients with malignant cancer	79	92	13.3 ± 17.0	7.0	0–82	54	21.7 ± 98.4	1.0	0–682

Although CTCs are found in 75% of patients with stage IV cancer, only a small percent of patients with stage I and II cancer were positive for CTCs. CAMLs were found in most patients with stage III–IV cancer and were found twice as often as CTCs in samples from patients with stage I/II cancer. In line with previous publications on CTCs, both the mean and the median CTC numbers increase dramatically as cancer stage progresses from stage I to stage IV. The CAML count also increases as cancer stage progresses. However CTC numbers are highly variable among patients. CAMLs seem to appear in all stages of cancer with a higher mean than CTCs. The presence and number of CAMLs seem to increase dramatically in patients undergoing chemotherapy treatment. No correlation was found between the number of CTCs and the number of CAMLs (Pearson's $r = 0.0728$, $P = 0.5235$ using a Student t test distribution).

Table S2. Summary of data for healthy subjects and for CAML$^+$ patients and CTC$^+$ patients separated by cancer type

Cancer type	No. of patients	CAML$^+$, %	Mean CAML± SD	Median CAML	CAML range	CTC$^+$, %	Mean CTC ± SD	Median CTC	CTC range
Healthy normal subjects	28	0	0 ± 0	0	0–0	0	0 ± 0	0	0–0
Nonmalignant	2	0	0 ± 0	0	0–0	0	0 ± 0	0	0–0
Breast (IBC)	14	93	24.9 ± 24.0	23.5	0–82	71	11.4 ± 28.1	3	0–108
Breast (IDC)	8	100	15.9 ± 16.1	10.5	1–41	100	9.0 ± 17.0	3.5	1–51
Breast (unknown)	7	100	15.0 ± 14.2	8	2–32	71	106.3 ± 254.2	5	0–682
Prostate	22	86	9.0 ± 13.6	4.5	0–64	41	3.1 ± 7.6	0	0–34
Pancreatic	28	93	9.7 ± 14.2	5.5	0–72	43	24.0 ± 104.5	0	0–541
Total patients with malignant cancer	79	92	13.3 ± 17.0	7.0	0–82	54	21.7 ± 98.4	1.0	0–682

CTCs were more common in patients with breast cancer and were found less often in patients with prostate or pancreatic cancers, probably because 26 of the 29 breast patients had late-stage (III or IV) disease. CAMLs were found at high rates in all three cancer types but were lowest in prostate cancer, probably because 15 of the 22 patients with prostate cancer had stage I or II disease. IBC, inflammatory breast cancer; IDC, invasive ductal carcinoma.

Table S3. Summary of cell markers used in the assays

Cell type	PDX-1	PSMA	CD11c	CD14	CD146	TIE-2 (C202b)	Cytokeratin 8,18, and 19	EpCAM (CD326)	CD45 (LCA)
CAML	+,*	+, ‡	+	+/–	+/–	+/–	+	+	+/–
Breast CTC	—	—	—	—	—	—	+	+/–	—
Prostate CTC	—	+	—	—	—	—	+	+/–	—
Pancreas CTC	+	—	—	—	—	—	+	+/–	—
Epithelial cell	—	—	—	—	—	—	+	+	—
Monocyte	—	—	+	+	–, §	–, §	—	—	+
Endothelial cell	—	—	—	—	+	+	+	—	—
Megakaryocyte	—	—	—	—	—	—	—	—	+/–
White blood cell	—	—	–, †	–,†	—	—	—	—	+

+, Positive in the majority of cell types. –, Negative in the majority of cell types. +/–, Cell populations are heterogeneous for this marker and may be positive or negative. *, Found only in cells from pancreatic cancer patients. ‡, Found only in cells from prostate cancer patients. §, A small subset population of monocytes are positive for this marker. †, Monocytes are a subpopulation of WBCs and commonly express the CD45 marker.

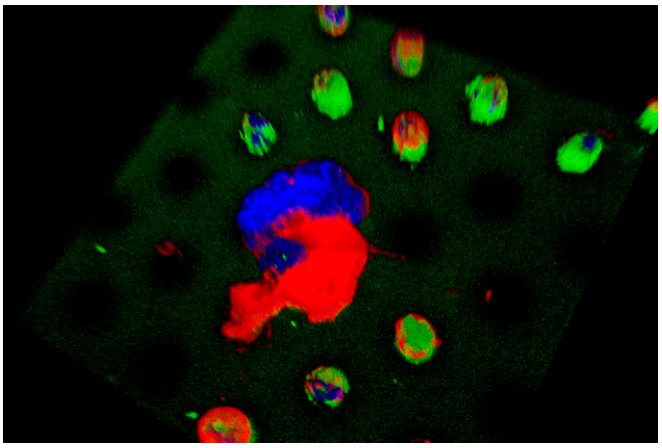

Movie S1. 3D representation of a CAML bound to a CTC. The interacting CAML and CTC from Fig. S4 were imaged by a confocal microscope to determine the full association between a CAML and a CTC. Anti-cytokeratin (green) overexposure is used to show the microfilter backdrop and the size of typical WBCs and to determine the x/y/z placement of the cells. DAPI staining (blue) shows the multinucleated structure of the CAML. The higher sensitivity of the confocal microscope allowed us to visualize the (red) protrusions from the CTC and show that these protrusions appear to be entwined with the CAML. The cross-reaction of the α-tubulin in the WBCs is caused by the high exposures needed to visualize the CTC protrusions.

Movie S1